Refractive Index Measurements of Films with Biaxial Symmetry. 2. Determination of Film Thickness and Refractive Indices Using Polarized Transmission Spectra in the Transparent Wavelength Range

Jie Diao and Dennis W. Hess*

School of Chemical and Biomolecular Engineering, Georgia Institute of Technology, Atlanta, Georgia 30332-0100

Received: August 18, 2004; In Final Form: May 4, 2005

A technique is formulated to determine both thickness and refractive indices of free-standing films with biaxial symmetry from polarized transmission spectra. The films must be transparent and show little dispersion in refractive indices in the wavelength range where the transmission spectra are collected. Methods are proposed to correct the errors caused by imperfect polarization of incident radiation and thickness variation across the sampling area. Anisotropic refractive indices and thickness of poly(biphenyl dianhydride-*p*-phenylenediamine) films which exhibit uniaxial optical anisotropy are determined from polarized transmission spectra. The refractive index and thickness values compare well to those obtained from waveguide prism coupler and profilometer measurements.

1. Introduction

Many techniques have been reported that can be used to determine the thickness and birefringent refractive indices of transparent anisotropic films, such as refractometry,[1] waveguide prism coupler,[1] variable-angle single wavelength ellipsometry,[2,3] spectroscopic ellipsometry,[4] surface plasmon resonance spectroscopy,[5,6] polarizing interference microscope[7] and methods based on polarized transmittance or reflectance.[8−14] Since collection of transmission and reflection spectra is routine in many laboratories, methods that use transmission or reflection spectra to extract anisotropic complex refractive indices are of special interest. Among the methods based on polarized transmission and reflection spectra, some use laser sources and generate refractive index values at particular wavelengths[8−10] and others use a common collimated light source and calculate the refractive index values based on polarized transmission or reflection spectra collected over a wavelength range.[12,13] With laser beams, it is possible to achieve high polarization efficiency while maintaining strong intensity. The small size (∼1 mm) of a laser beam also limits the influence of sample nonuniformity in extracting refractive indices and film thickness. However, for a common collimated light source, such as a white light or an infrared source, usually the beam size is large to achieve satisfactory beam intensity. Since polarizers are used to change the polarization state of the light, polarization efficiency can be compromised by a drop in light intensity due to absorption by the polarizers. Both imperfect polarization and sample nonuniformity across the light beam may lead to errors when extracting refractive indices and film thickness from the polarized spectra. Nevertheless, few approaches have been proposed to correct for these errors. In the following, a technique is proposed to determine both anisotropic refractive indices and thickness of a film with biaxial symmetry based on polarized transmission spectra collected at oblique incidence over a wavelength range where the film is transparent and shows little dispersion in refractive indices. Methods are indicated to correct the errors caused by imperfect polarization of incident radiation and thickness variation across the sampling area.

* Corresponding author. Tel.: +1-404-894-5922. Fax: +1-404-894-2866. E-mail: dennis.hess@chbe.gatech.edu.

2. Theory

2.1. Transmittance and Reflectance of p-Polarized and s-Polarized Light. When light impinges on a free-standing film in air at an incident angle of θ in the *XZ* plane (Figure 1), the transmittance of p-polarized (T_p) and s-polarized (T_s) light can be calculated from the following equations:[15]

$$1/T_p = \left|\left(\frac{1}{2} + \frac{H}{4} + \frac{1}{4H}\right)\exp[i\gamma_1 t] + \left(\frac{1}{2} - \frac{H}{4} - \frac{1}{4H}\right) \times \exp[-i\gamma_1 t]\right|^2 \quad (1)$$

$$1/T_s = \left|\left(\frac{1}{2} + \frac{G}{4} + \frac{1}{4G}\right)\exp[i\gamma_3 t] + \left(\frac{1}{2} - \frac{G}{4} - \frac{1}{4G}\right) \times \exp[-i\gamma_3 t]\right|^2 \quad (2)$$

where

$$H = \frac{{n_0}^2\sqrt{(n_z - ik_z)^2 - \sin^2\theta}}{(n_x - ik_x)(n_z - ik_z)\sqrt{{n_0}^2 - \sin^2\theta}} \quad (3)$$

$$G = \frac{\sqrt{{n_0}^2 - \sin^2\theta}}{\sqrt{(n_y - ik_y)^2 - \sin^2\theta}} \quad (4)$$

$$\gamma_1 = (\omega/c)\frac{(n_x - ik_x)}{(n_z - ik_z)}\sqrt{(n_z - ik_z)^2 - \sin^2\theta} \quad (5)$$

$$\gamma_3 = (\omega/c)\sqrt{(n_y - ik_y)^2 - \sin^2\theta} \quad (6)$$

In deriving eqs 1−6, the film is assumed to possess any degree of anisotropy up to and including full biaxial symmetry

10.1021/jp0462761 CCC: $30.25
Published on Web 06/10/2005

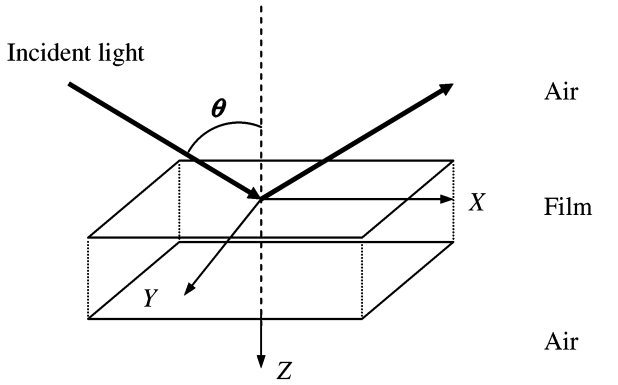

Figure 1. Geometry of electromagnetic wave propagation in a free-standing film in air.

(with the symmetry axes coinciding with *X*, *Y*, and *Z* axes). n_x, n_y, and n_z and k_x, k_y, and k_z are the *X*, *Y*, and *Z* components of refractive index (n) and extinction coefficient (k), respectively. n_0 is the refractive index of air, t the film thickness, ω the frequency of incident light, and c the speed of light in a vacuum.

By setting $k_x = k_y = k_z = 0$ in eqs 1−6, we can obtain T_s and T_p for a biaxial transparent film

$$T_p = \frac{1}{1 + (4C^2 - 1)\sin^2\left(\frac{\omega n_x \sqrt{n_z^2 - \sin^2\theta}}{c n_z} t\right)} \quad (7)$$

$$T_s = \frac{1}{1 + (4D^2 - 1)\sin^2\left(\frac{\omega \sqrt{n_y^2 - \sin^2\theta}}{c} t\right)} \quad (8)$$

where

$$C = \frac{n_0^2 \sqrt{n_z^2 - \sin^2\theta}}{n_x n_z \sqrt{n_0^2 - \sin^2\theta}} + \frac{n_x n_z \sqrt{n_0^2 - \sin^2\theta}}{n_0^2 \sqrt{n_z^2 - \sin^2\theta}} \quad (9)$$

$$D = \frac{\sqrt{n_0^2 - \sin^2\theta}}{\sqrt{n_y^2 - \sin^2\theta}} + \frac{\sqrt{n_y^2 - \sin^2\theta}}{\sqrt{n_0^2 - \sin^2\theta}} \quad (10)$$

2.2. Correction for Polarizer Efficiency. Experimental errors will be introduced to the polarized transmission spectra if the incident light polarization is not perfect. It is important that the influence of imperfect polarization on transmittance be properly addressed and related errors be corrected. In the following discussion, $I_{||}$ denotes the intensity of polarized light parallel to the polarizer electric vector direction and $I_\perp$ denotes the intensity of polarized light perpendicular to the polarizer electric vector direction. Note that both $I_{||}$ and $I_\perp$ refer to intensities after the light passes through the polarizer but before striking the sample. q is defined as the fraction of polarized light intensity parallel to the polarizer electric vector direction

$$q = \frac{I_{||}}{I_{||} + I_\perp} \quad (11)$$

q is a function of both the polarization state of incoming infrared radiation and the polarization efficiency of the polarizer. (Appendix I presents a more detailed discussion on the relation between q and polarizer efficiency.) For light passing an ideal polarizer, $q = 1$; for randomly polarized light, $q = 0.5$. If the polarizer used for spectra collection is not perfect, the measured transmittance for s- or p-polarized light will generally be a mixture of transmittance from both s-polarized and p-polarized light. Thus, the measured transmittance for s- and p-polarized light can be expressed by

$$T_{s,measured} = \frac{I_{||}T_s + I_\perp T_p}{(I_{||} + I_\perp)} = qT_s + (1 - q)T_p \quad (12)$$

$$T_{p,measured} = \frac{I_{||}T_p + I_\perp T_s}{(I_{||} + I_\perp)} = qT_p + (1 - q)T_s \quad (13)$$

If the polarization state of incoming infrared radiation is well characterized and the dependence of polarizer efficiency on wavelength is known, T_s and T_p can be extracted from $T_{s,measured}$ and $T_{p,measured}$ using eqs 12 and 13. In practice, the dependence of polarizer efficiency on wavelength can be obtained through calibration. However, due to reflections from the mirror sets in the spectrometer, the incoming infrared radiation is not randomly polarized prior to striking the polarizer; as a result, the polarization state is generally unknown. Therefore, estimation of q is difficult. If the experimental error caused by q is not properly taken into account, significant error may result when the polarized transmission spectra are used to extract physical characteristics of the film. In the following, we propose a technique to eliminate errors caused by q by invoking a simple algebraic manipulation. Adding eq 12 to eq 13 yields

$$T_{p,measured} + T_{s,measured} = T_p + T_s \quad (14)$$

Equation 14 indicates that the influence of q will be eliminated if the sum of p- and s-polarized transmittance is used in calculation.

2.3. Correction for Sample Thickness Variation. If the sample is uniform in thickness and if no refractive index dispersion exists over the wavelength range, the polarized transmittance should exhibit exact periodic oscillation with respect to wavelength as indicated by eqs 7 and 8. The transmittance is also expected to be equal to 1 at certain wavelengths. However, if the thickness varies across the sample area, the oscillation will not be ideally periodic and the transmittance is unlikely to reach a value of 1 at any wavelength. This deviation from ideality can cause significant error in determining the refractive index and thickness if the thickness variation is not taken into account.

In practice, the influence of thickness variation will be convoluted with the nonuniformity in intensity of incident radiation. If $f(t)$ denotes the thickness distribution function in the illuminated sample area, i.e., if the percentage of film area with thicknesses falling within the range $[t, t + dt]$ can be represented by $f(t)\,dt$, then

$$\int_{t_{min}}^{t_{max}} f(t)\,dt = 1 \quad (15)$$

where t_{min} and t_{max} are the minimum and maximum thickness in the illuminated sample area, respectively. For commercial infrared spectrometers, radiation from the infrared source after reflections from a series of mirrors is not likely to have uniform intensity across the illuminated area. If we assume that the percentage of radiation intensity striking an area with thicknesses falling within the range $[t, t + dt]$ can be represented by $f'(t)\,dt$, then

$$\int_{t_{min}}^{t_{max}} f'(t)\,dt = 1 \quad (16)$$

In the following discussion, $f'(t)$ is called the intensity weighted thickness distribution function. If the intensity of incoming radiation is not uniform, $f(t)$ and $f'(t)$ will be different. For a total intensity (I) of radiation striking the sample, the transmittance after thickness variation correction ($T_{\Delta t}$) will be

$$T_{\Delta t} = \frac{\int_{t_{min}}^{t_{max}} I\, f'(t)\, T(t)\, dt}{I} = \int_{t_{min}}^{t_{max}} f'(t)\, T(t)\, dt \qquad (17)$$

where $T(t)$ is the transmittance if the sample has a uniform thickness t. According to eq 17, it is the intensity weighted thickness distribution function instead of the actual thickness distribution function that determines the measured transmittance. Experimental determination of $f'(t)$ may be difficult given the fact that thickness variation and intensity nonuniformity of incident radiation are linked. In this paper, we correct the transmittance error caused by $f'(t)$ by making the simple assumption that $f'(t)$ is a uniform distribution function

$$f'(t) = \frac{1}{t_{max} - t_{min}} \qquad t_{min} < t < t_{max} \qquad (18)$$

Substitution of eqs 7 and 18 into eq 17 gives

$$\begin{aligned} T_{p,\Delta t} &= \int_{t_{min}}^{t_{max}} f'(t)\, T_p(t)\, dt \\ &= \int_{t_{min}}^{t_{max}} \frac{1/(t_{max} - t_{min})}{1 + (4C^2 - 1)\sin^2\left(\frac{\omega n_x \sqrt{n_z^2 - \sin^2\theta}}{c n_z} t\right)} dt \\ &= \frac{\arctan\left[2C \tan\left(\frac{\omega n_x \sqrt{n_z^2 - \sin^2\theta}}{c n_z} t_{max}\right)\right]}{2C\frac{\omega n_x \sqrt{n_z^2 - \sin^2\theta}}{c n_z}} - \\ &\qquad \frac{\arctan\left[2C \tan\left(\frac{\omega n_x \sqrt{n_z^2 - \sin^2\theta}}{c n_z} t_{min}\right)\right]}{2C\frac{\omega n_x \sqrt{n_z^2 - \sin^2\theta}}{c n_z}} \end{aligned} \qquad (19)$$

Similarly

$$\begin{aligned} T_{s,\Delta t} &= \int_{t_{min}}^{t_{max}} f'(t)\, T_s(t)\, dt \\ &= \int_{t_{min}}^{t_{max}} \frac{1/(t_{max} - t_{min})}{1 + (4D^2 - 1)\sin^2\left(\frac{\omega \sqrt{n_y - \sin^2\theta}}{c} t\right)} dt \\ &= \frac{\arctan\left[2D \tan\left(\frac{\omega \sqrt{n_y^2 - \sin^2\theta}}{c} t_{max}\right)\right]}{2D\frac{\omega \sqrt{n_y^2 - \sin^2\theta}}{c}} - \\ &\qquad \frac{\arctan\left[2D \tan\left(\frac{\omega \sqrt{n_y^2 - \sin^2\theta}}{c} t_{min}\right)\right]}{2D\frac{\omega \sqrt{n_y^2 - \sin^2\theta}}{c}} \end{aligned} \qquad (20)$$

It should be pointed out that function "arctan" only has values within the range $[-\pi/2, \pi/2]$; thus in eqs 19 and 20, at certain wavelengths, the acrtan function will be discontinuous (sudden change from $\pi/2$ to $-\pi/2$, or from $-\pi/2$ to $\pi/2$). Because such discontinuities in the first term and the second term are unlikely to occur at the same wavelength, calculations can be adjusted by adding or subtracting π from the first term to make $T_{\Delta t}$ a continuous function with respect to wavelength.

In this paper, we demonstrate the use of eqs 7 and 8 to determine both thickness and anisotropic refractive indices from polarized transmission spectra and describe the correction of errors due to imperfect polarization and nonuniformity in sample thickness. It has been widely reported that spin-coated poly(biphenyl dianhydride-*p*-phenylenediamine) (BPDA-PDA) films exhibit uniaxial optical anisotropy.[16−19] A previous ultraviolet−visible (UV−vis) and infrared (IR) absorption study suggested that BPDA-PDA films are transparent in the wavelength range between 1.5 and 2.5 μm (corresponding to ∼6600−4000 cm^{-1}) and show little dispersion in refractive index.[17] In the following, we extract both thickness and anisotropic refractive indices from the transmission spectra between 4500 and 6000 cm^{-1}. The wavelength range between 4000 and 4500 cm^{-1} has been excluded in order to minimize the influence of water vapor absorption near 4000 cm^{-1} on the transmission spectra. Thickness values obtained with the method described in this paper can be used as an input to determine complex refractive indices in the absorbing wavelength range with the R/T ratio method.[15]

3. Experimental Procedures

3.1. Film Preparation. BPDA-PDA (PI2611) was obtained from HD Microsystems, Inc., in the poly(amic acid) form dissolved in *N*-methyl pyrrolidone (NMP); this solution was used as received. Four-inch silicon wafers were spin coated (3000 rpm) with an adhesion promoter (VM652 from HD Microsystems, Inc.) and heated on a hot plate at 110 °C for 1 min, followed by poly(amic acid) spin coating at 5000 rpm. The films were soft baked at 90 °C for 1.5 min and hard baked at 150 °C for 1.5 min to remove most of the NMP solvent. Subsequently, the films were cured in nitrogen at 350 °C for 30 min with a temperature ramp rate of 4 °C/min. The BPDA-PDA film thickness after curing measured by the profilometer was ∼3.5 μm. After curing, the front (polyimide) side of the wafer was protected by spin coating a thin layer of photoresist (AZ P4620 from Clariant, Inc.). Subsequently, 1 cm diameter circular openings were fabricated on the silicon wafer with a backside patterning and etching process.[15] As a result of this procedure, the BPDA-PDA film over the openings was free-standing. In this study, six 2 cm × 2 cm sample films with 1 cm diameter circular opening were cut from a single silicon wafer and were designated as #1 to #6 in the following discussion. The free-standing BPDA-PDA films were then dry-etched in a Plasma-Therm reactive ion etcher to produce a series of films with the same optical anisotropy but with different thicknesses.[19] The corresponding etch times for films #1, #2, #3, #4, #5, and #6 are 0, 60, 150, 270, 390, and 0 s, respectively. Films #1 and #6 are in different areas on the wafer but went through identical process steps.

3.2. FTIR Measurement. The infrared spectra were collected on a Bruker Equinox 55 infrared spectrometer equipped with a deuterated triglycine sulfide (DTGS) detector. All spectra were taken at 2 cm^{-1} resolution, 512 scans in the wavelength range of 400∼6000 cm^{-1}. The polarization state of incident light was adjusted by using both a Harrick KRS-5 wire grid polarizer and a Perkin-Elmer wire grid polarizer; two polarizers were used

side-by-side in series to increase the polarization efficiency. Variable incident angle transmission spectra were collected with a modified variable angle reflection stage. Details of the spectra collection configuration can be found in ref 15.

3.3. Waveguide Prism Coupler and Profilometer Measurement. The refractive indices of cured polyimide films were measured in air using a prism coupler (Metricon, model 2010) equipped with a laser light source at 1550 nm (corresponding to 6450 cm^{-1}). The resolution of the refractive index was ± 0.0005 and that of the film thickness was $\pm 0.3\%$ over the 0.5−15 μm thickness range. The BPDA-PDA film thickness was also measured with a Tencor Alpha Step profilometer. Both the prism coupler and profilometer measurements were performed in a region close to the circular opening.

4. Data Analysis

Since spin coated BPDA-PDA films exhibit uniaxial optical anisotropy,[16−19] equality of n_x and n_y values were assumed in all calculations. The dispersion of refractive indices in the wavelength range between 4500 and 6000 cm^{-1} was neglected. It was further assumed that $f'(t)$ would follow the uniform distribution function described by eq 18; the four unknown parameters (n_x, n_z, t_{max}, and t_{min}) were determined from the s- and p-polarized transmission spectra using least squares regression. The parameters $\bar{t}$ and Δt, defined by eqs 21 and 22, replaced the two parameters t_{max} and t_{min}

$$\bar{t} = \frac{t_{max} + t_{min}}{2} \tag{21}$$

$$\Delta t = \frac{t_{max} - t_{min}}{2} \tag{22}$$

$\bar{t}$ and Δt can be viewed as intensity weighted average thickness and intensity weighted half thickness span. A Matlab 6.x function "fminsearch" was used to find the optimal parameters by minimizing the following target function $g(n_x,n_z,\bar{t},\Delta t)$:

$$g(n_x,n_z,\bar{t},\Delta t) = \sum (T_{p,\Delta t} + T_{s,\Delta t} - T_{p,measured} - T_{s,measured})^2 \tag{23}$$

which is the sum of squared error over the wavelength range. $T_{p,\Delta t}$ and $T_{s,\Delta t}$ were determined from eqs 19 and 20, respectively; the function "fminsearch" uses a simplex search method.[20]

For comparison purposes, two additional target functions: $g'(n_x,n_z,\bar{t},\Delta t)$ and $g''(n_x,n_z,\bar{t})$ were defined as

$$g'(n_x,n_z,\bar{t},\Delta t) = \sum \lfloor (T_{p,\Delta t} - T_{p,measured})^2 + (T_{s,\Delta t} - T_{s,measured})^2 \rfloor \tag{24}$$

and

$$g''(n_x,n_z,\bar{t}) = \sum (T_p + T_s - T_{p,measured} - T_{s,measured})^2 \tag{25}$$

respectively, where $T_{p,\Delta t}$, $T_{s,\Delta t}$, T_p, and T_s were calculated from eqs 19, 20, 7, and 8, respectively. Determination of $n_x,n_z,\bar{t}$ and Δt by minimizing $g'(n_x,n_z,\bar{t},\Delta t)$ corresponds to the inclusion of thickness variation but neglect of imperfect polarization, while determination of $n_x,n_z,\bar{t}$ by minimizing $g''(n_x,n_z,\bar{t})$ corresponds to inclusion of imperfect polarization while neglecting thickness variation.

In the following discussion, refractive indices and film thicknesses measured by the prism coupler and profilometer (thickness only) are also reported for comparison purposes. It is worth mentioning that the prism coupler technique utilizes a high quality laser source and samples an area approximately equal to the size of the laser beam (~1 mm) so that excellent accuracy is possible. For the method described in this paper, unless an intense radiation source is used and the sampling area is small, it is very difficult to achieve the accuracy obtainable with the prism coupler. We estimate that the error for n_x, n_z, and $\bar{t}$ will be ± 0.05, ± 0.1, and ± 0.1 μm, respectively. In this paper, all refractive indices and film thicknesses (in μm) determined with the transmission spectra are reported to the second decimal point. Refractive indices obtained by the prism coupler are reported to the third decimal point. Because the thickness can vary up to several tenths of a micron across the sample, all thickness values (in μm) from the prism coupler and profilometer are reported to the second decimal point.

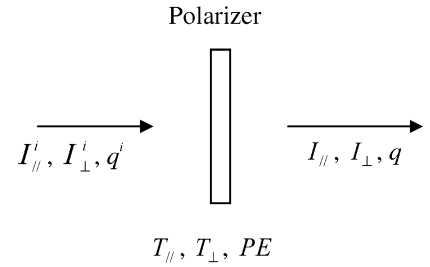

Figure 2. Schematic representation of light passing through a polarizer.

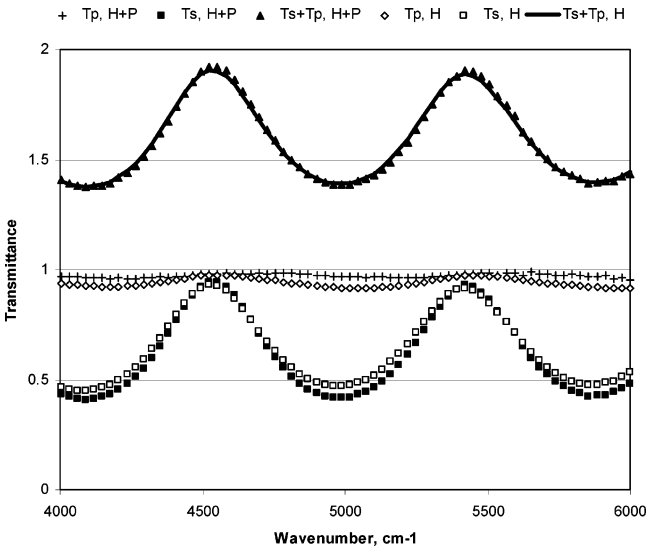

Figure 3. Comparison between transmission spectra collected with a Harrick polarizer only and with a Harrick and a Perkin-Elmer polarizer used in series (spectra are collected at 56° incident angle on identical sample area).

5. Results and Discussion

5.1. Corrections for Imperfect Polarization. Both the Harrick KRS-5 wire grid polarizer and the Perkin-Elmer wire grid polarizer possess high polarization efficiency in the mid infrared range (>0.95 at 2000 cm^{-1}). The polarizer efficiency is lower in the wavelength range between 4500 and 6000 cm^{-1}. Therefore, significant error can result unless corrections are made for imperfect polarization. A common method of enhancing polarization efficiency is to use two polarizers in series and align their electric vector directions parallel to each other. Figure 3 compares the transmission spectra collected with the Harrick polarizer only ($T_{s,H}$, $T_{p,H}$, $T_s + T_{p,H}$) and with the Harrick and the Perkin-Elmer polarizer in series ($T_{s,H+P}$, $T_{p,H+P}$, $T_s + T_{p,H+P}$). The difference between $T_{s,H}$ and $T_{s,H+P}$ (or between $T_{p,H}$ and

TABLE 1: Effect of Imperfect Polarization on Calculated Optical Constants and Film Thickness[a]

			calculation results			
polarizer	correction for imperfect polarization?	target function	n_x	n_z	$\bar{t}$, μm	Δt, μm
Harrick only	yes	$g(n_x,n_z,\bar{t},\Delta t)$	1.80	1.52	3.46	0.09
	no	$g'(n_x,n_z,\underline{t},\Delta t)$	1.70	1.18	3.74	0.11
Harrick and Perkin-Elmer in series	yes	$g(n_x,n_z,\underline{t},\Delta t)$	1.80	1.52	3.47	0.08
	no	$g'(n_x,n_z,t,\Delta t)$	1.77	1.52	3.54	0.08
prism coupler results			1.779	1.598	3.54	
profilometer results					3.50	

[a] Based on transmission spectra collected at 56° incident angle on sample film #1.

TABLE 2: Refractive Indices and Film Thickness Determined with and without Correction for Thickness Variation[a]

			calculation results				prism coupler			profilometer
#	correction for thickness variation?	target function	n_x	n_z	$\bar{t}$, μm	Δt, μm	n_x	n_z	t, μm	t, μm
1	yes	$g(n_x,n_z,\bar{t},\Delta t)$	1.78	1.56	3.50	0.08	1.779	1.598	3.54	3.50
	no	$g''(n_x,n_z,\underline{t})$	1.77	1.48	3.54					
2	yes	$g(n_x,n_z,\underline{t},\Delta t)$	1.78	1.56	3.32	0.05	1.779	1.599	3.21	3.40
	no	$g''(n_x,n_z,\underline{t})$	1.78	1.52	3.34					
3	yes	$g(n_x,n_z,\underline{t},\Delta t)$	1.80	1.53	2.89	0.05	1.780	1.600	2.79	2.87
	no	$g''(n_x,n_z,\underline{t})$	1.79	1.49	2.90					
4	yes	$g(n_x,n_z,\underline{t},\Delta t)$	1.78	1.51	2.36	0.03	1.779	NA[b]	2.15	2.22
	no	$g''(n_x,n_z,\underline{t})$	1.77	1.49	2.36					
5	yes	$g(n_x,n_z,\underline{t},\Delta t)$	1.79	1.50	1.79	0.04	NA[b]	NA[b]	NA[b]	1.65
	no	$g''(n_x,n_z,t)$	1.78	1.45	1.80					

[a] Based on transmission spectra collected at 45° incident angle. [b] The data were not available because the films are too thin for the prism coupler to generate enough modes for accurate parameter determination.

$T_{p,H+P}$) is apparent. The mixing of signals between T_s and T_p with the Harrick polarizer only is more significant as compared to that with two polarizers in series. However, the sum of T_s and T_p is relatively insensitive to whether one or two polarizers are used, which validates eq 14.

Table 1 shows the results of refractive index and thickness calculations when only the Harrick polarizer was used and when the Harrick and Perkin-Elmer polarizers were used in series. For comparison, measurement results on the same sample by the prism coupler and profilometer are also shown in Table 1. We have established that the refractive indices are uniform ($\pm$0.001) across a film on a single wafer although the film thickness can differ up to 0.4 μm for an average thickness of 3 μm.[19] Thus, the refractive index values measured by the prism coupler are the accurate values for comparison to the calculated n_x and n_z, whereas either the thickness measured by the prism coupler or the profilometer can be used as estimated references for a calculated $\bar{t}$. Clearly, for measurements with the Harrick polarizer only, if no correction for imperfect polarization is made, the calculated refractive indices and thickness values can differ significantly from those obtained by the prism coupler and profilometer. If the imperfect polarization is corrected, results with the Harrick polarizer only and with the two polarizers in series are very close; calculated n_x and $\bar{t}$ values match those from the prism coupler and profilometer measurements better than the calculated n_z values. This is understandable because the interference pattern displayed by T_s in Figure 3 is more obvious than that displayed by T_p. As shown by eqs 7 and 8, T_s is solely determined by n_x, whereas T_p is determined by both n_z and n_x. Therefore, the calculated n_x values are expected to be more accurate than the calculated n_z values.

From Table 1, it can also be seen that, when two polarizers are used in series, the calculation results are essentially independent of whether the imperfect polarization was corrected or not. This is a result of improved polarization efficiency with two polarizers in series. By reconstructing the T_s and T_p spectra with calculated n_x,n_z,$\bar{t}$ and Δt values, an estimate of the polarizer efficiency in the 4500$-$6000 cm^{-1} wavelength range could be obtained: $\sim$0.88 for the Harrick polarizer and $\sim$0.97 for the two polarizers in series. Although additional polarizers in series can improve the polarization efficiency, this will also significantly reduce the incident radiation intensity due to polarizer absorption and reflection, which may result in lower signal/noise ratio for the intensity measurements. Therefore, the polarization efficiency and intensity signal/noise ratio must be carefully balanced. It is recommended that the correction for imperfect polarization be made even if high polarizer efficiency can be obtained because any misalignment between the polarizer electric vector direction and Y (or Z) axis will have a similar effect to that of an imperfect polarizer.

5.2. Corrections for Sample Thickness Variation. Color fringes are observed across the 4-in. diameter wafer after spin coating and curing of the BPDA-PDA film, which is an indication of thickness nonuniformity. The thickness generally decreases from the center to the edge of the wafer; the thickness variation is more significant near the edge of the wafer. Profilometer measurements were performed on 2 cm $\times$ 2 cm pieces cut from the wafer and the maximum thickness variation was as high as 0.3 μm (from 3.35 to 3.65 μm). The sampling areas in transmission spectra collection are circles with a diameter of $\sim$1 cm; therefore, the thickness variation can be as large as 0.15 μm (or $\Delta t = 0.7\sim0.8$ μm). The reactive ion etching rates of BPDA-PDA film may also be different across the sample, which may increase or decrease the thickness variation caused by the spin coating process. It is thus important that thickness variation be considered and appropriately corrected.

Table 2 shows the refractive indices and film thicknesses for sample films #1 to #5 with thickness variation corrected and uncorrected. The calculated average thickness values do not change significantly with or without the thickness variation correction. However, the calculated n_x and n_z values, and especially n_z values, are less accurate if the thickness variation is not corrected. The calculated Δt values fall into the range of 0.03$-$0.07 μm, which is comparable to the expected thickness variation magnitude. Again, it is important to note that Δt is the intensity weighted half thickness span for a simplified distribution model described by eq 18.

TABLE 3: Refractive Indices and Film Thickness Determined from Transmission Spectra Collected at Different Incident Angles

			calculation results			
sample #	incident angle	target function	n_x	n_z	$\bar{t}$, μm	Δt, μm
1	0°	$g(n_x,n_z,\bar{t},\Delta t)$[a]	1.78	/	3.51	0.07
	45°	$g(n_x,n_z,\bar{t},\Delta t)$	1.78	1.56	3.50	0.08
	56°	$g(n_x,n_z,\bar{t},\Delta t)$	1.80	1.52	3.47	0.08
6	45°	$g(n_x,n_z,\bar{t},\Delta t)$	1.79	1.57	3.50	0.06
	56°	$g(n_x,n_z,t,\Delta t)$	1.77	1.50	3.51	0.08

[a] For 0° incident angle, n_z will have no effect on the transmittance. Therefore, only T_s will be considered in the target function. The polarization state of incident radiation will not influence the transmittance because of the in-plane isotropy of the film.

From Table 2, it can also be seen that, as the films become thinner, the calculated n_z values deviate further from the true values. We attribute this to experimental error related to thickness change. Interference patterns for thick films usually show at least one complete cycle in the wavelength range (Figure 3); the periodicity exhibited by the complete interference wave will aid the computer search algorithm to converge on the correct thickness and refractive index values. However, as the films become thinner, only incomplete cycles are obtained, which leads to more error in determining the periods of oscillation and ultimately the refractive index and thickness values. Oscillation in interference patterns of p-polarized light is not as obvious as that in interference patterns of s-polarized light. Therefore, the lack of a complete wave will have a larger impact on p-polarized light relative to s-polarized light; the error in calculated n_z values thus becomes more significant as the films become thinner.

5.3. Results from Different Incident Angles. Table 3 shows the results of refractive index and thickness calculation based on transmission spectra of sample #1 collected at difference incident angles: 0°, 45°, and 56°. At 0° incident angle, the difference between s- and p-polarized light disappears and only T_s is considered in calculating the transmittance; therefore, only n_x values are reported. These results indicate that the calculated refractive index and thickness values do not change significantly with incident angle. As the incident angle changes, the relative position of the sample in the light path changes and the thickness will be weighted differently by the incident intensity. Therefore, small changes in the intensity weighted thickness and half thickness span are expected. Also, a change in incident angle leads to a change in the magnitude of oscillation in the interference patterns of both s- and p-polarized light, which influences the accuracy of the calculation. Films #1 and #6 are in different areas on the wafer but went through identical processing steps. For comparison, the calculation results based on transmission spectra of sample #6 collected at 45° and 56° incident angles are also shown in Table 3. As expected, the refractive index and thickness values obtained for film #6 are similar to those for film #1.

6. Conclusions

A technique has been proposed to determine both anisotropic refractive indices and thickness of a film with biaxial symmetry based on polarized transmission spectra collected at oblique incidence over the wavelength range where the film is transparent and shows little dispersion in refractive indices. The influence of imperfect polarization of incident light and thickness variation across the sample on the measured transmittance and reflectance is discussed and methods are proposed to correct the error caused by imperfect polarization and thickness variation. Anisotropic refractive indices and thickness of BPDA-PDA films are determined from polarized transmission spectra collected in the wavelength range between 4500 and 6000 cm^{-1}. If imperfect polarization and thickness variation are not taken into account, significant errors may result in the calculation of refractive indices and thicknesses. The estimated refractive index and thickness values compare well to those obtained from waveguide prism coupler and profilometer measurements after proper corrections are made.

Appendix I. Relation between Polarizer Efficiency (PE) and Fraction of Polarized Light Intensity Parallel to the Polarizer Electric Vector Direction (q)

Polarizer efficiency (PE), or degree of polarization, is defined as[21]

$$\mathrm{PE}(\nu) = \frac{T_{\parallel}(\nu) - T_{\perp}(\nu)}{T_{\parallel}(\nu) + T_{\perp}(\nu)} \tag{26}$$

where $T_{\parallel}(\nu)$ is the transmittance at wavelength ν when the polarizer electric vector direction is aligned parallel to a fully polarized beam and $T_{\perp}(\nu)$ is the transmittance at wavelength ν when the polarizer electric vector direction is aligned perpendicular to the fully polarized beam. Figure 2 schematically shows light passing a polarizer. We use $I^i_{\parallel}$ and $I^i_{\perp}$ to denote the intensity component of the two directions (one parallel and the other perpendicular to the polarizer electric vector direction) of incident light prior to striking the polarizer. The corresponding fraction of polarized light intensity parallel to the polarized electric vector direction q^i is defined in a similar way as in eq 11

$$q^i = \frac{I^i_{\parallel}}{I^i_{\parallel} + I^i_{\perp}} \tag{27}$$

Therefore

$$I_{\parallel} = I^i_{\parallel} T_{\parallel} \tag{28}$$

$$I_{\perp} = I^i_{\perp} T_{\perp} \tag{29}$$

$$q = \frac{I^i_{\parallel} T_{\parallel}}{I^i_{\parallel} T_{\parallel} + I^i_{\perp} T_{\perp}} = \frac{I^i_{\parallel}/I^i_{\perp}}{I^i_{\parallel}/I^i_{\perp} + T_{\perp}/T_{\parallel}} = \frac{q^i + q^i \mathrm{PE}}{1 - \mathrm{PE} + 2q^i \mathrm{PE}} \tag{30}$$

Equation 30 relates q, q^i, and PE. If the light is randomly polarized before hitting the polarizer, $q^i = 0.5$. In this case, $q = (1 + \mathrm{PE})/2$. If the polarizer is an ideal polarizer (PE = 1) or the incident beam is fully polarized ($q^i = 1$), q will also be 1. In an infrared spectrometer, although the radiation produced by the infrared source tends to be randomly polarized, the randomness in polarization cannot be guaranteed when the radiation passes through the mirror sets in the spectrometer due to the difference in reflectivity of p- and s-polarized light on the mirrors. Therefore, in a common infrared spectrometer, q cannot be solely determined by PE; it depends on q^i as well.

Acknowledgment. The authors thank Professor Robert Samuels and Ms. Zhi Li for experimental assistance with the prism coupler measurements and Dr. Weontae Oh and Professor

Sankar Nair for access to the infrared spectrometer. We also thank Applied Materials for a fellowship for Jie Diao.

References and Notes

(1) Hardaker, S. S.; Moghazy, S.; Cha, C. Y.; Samuels, R. J. *J. Polym. Sci. Part B: Polym. Phys.* **1993**, *31*, 1951−1963.

(2) Krzyzanowska, H.; Kulik, M.; Zuk, J. *J. Lumin.* **1999**, *80*, 183−186.

(3) Matsuhashi, N.; Okumoto, Y.; Kimura, M.; Akahane, T. *Jpn. J. Appl. Phys. Part 1* **2002**, *41*, 4615−4619.

(4) Woollam, J. A.; Bungay, C.; Hilfiker, J.; Wiwald, T. *Nucl. Instrum. Methods B* **2003**, *208*, 35−39.

(5) Salamon, Z.; Macleod, H. A.; Tollin, G. *Biochim. Biophys. Acta* **1997**, *1331*, 117−129.

(6) Salamon, Z.; Macleod, H. A.; Tollin, G. *Biophys. J.* **1997**, *73*, 2791−2797.

(7) Sadik, A. M.; Ramadan, W. A.; Litwin, D. *Meas. Sci. Technol.* **2003**, *14*, 1753−1759.

(8) Surdutovich, G. I.; Kolenda, J.; Fragali, J. F.; Misoguti, L.; Vitlina, R.; Baranauskas, V. *Thin Solid Films* **1996**, *279*, 119−123.

(9) Basmaji, P.; Bagnato, V. S.; Grivickas, V.; Surdutovich, G. I.; Vitlina, R. *Thin Solid Films* **1993**, *223*, 131−136.

(10) Lee, S. W.; Kwon, S. Y.; Lee, H. *Macromol. Symp.* **1997**, *118*, 451−459.

(11) Yu, G.; Ishikawa, H.; Egawa, T.; Soga, T.; Watanabe, J. *Jpn. J. Appl. Phys. Part 2* **1997**, *36*, L1029−L1031.

(12) Martinez-Anton, J. C. *Mater. Lett.* **2002**, *53*, 117−121.

(13) Martinez-Anton, J. C. *Opt. Mater.* **2002**, *19*, 335−341.

(14) Kihara, T.; Yokomori, K. *Proc. SPIE* **1992**, *1746*, 259−268.

(15) Diao, J.; Hess, D. W. *J. Phys. Chem. B* **2005**, *109*, 12800−12818.

(16) Heminghaus, S.; Boese, D.; Yoon, D. Y.; Smith, B. A. *Appl. Phys. Lett.* **1991**, *59*, 1043−1045.

(17) Boses, D.; Lee, H.; Yoon, D. Y.; Swalen, J. D.; Rabolt, J. F. *J. Polym. Sci. Part B: Polym. Phys.* **1992**, *30*, 1321−1327.

(18) Lin, L.; Bidstrup, S. A. *J. Appl. Polym. Sci.* **1994**, *54*, 553−560.

(19) Diao, J.; Hess, D. W. *Thin Solid Films* **2005**, *483*, 226−231.

(20) Lagarias, J. C.; Reeds, J. A.; Wright, M. H.; Wright, P. E. *SIAM J. Optimiz.* **1998**, *9*, 112−147.

(21) Bennett, J. M.; Bennett, H. E. In *Handbook of Optics*; Driscoll, W. G., Vaughan, W., Eds.; McGraw-Hill: New York, 1978; Section 10.